Asia-Pacific Journal of Sports Medicine, Arthroscopy, Rehabilitation and Technology 40 (2025) 1–6

Contents lists available at ScienceDirect

Asia-Pacific Journal of Sports Medicine, Arthroscopy, Rehabilitation and Technology

journal homepage: www.ap-smart.com

Original article

Using deep learning for ultrasound images to diagnose chronic lateral ankle instability with high accuracy

Masamune Kamachi, Kohei Kamada, Noriyuki Kanzaki *, Tetsuya Yamamoto, Yuichi Hoshino, Atsuyuki Inui, Yuta Nakanishi, Kyohei Nishida, Kanto Nagai, Takehiko Matsushita, Ryosuke Kuroda

Department of Orthopaedic Surgery, Kobe University Graduate School of Medicine, Kobe, 650-0017, Japan

ARTICLE INFO

Keywords:
Anterior talofibular ligament
Artificial intelligence
Chronic lateral ankle instability
Deep learning
Ultrasound

ABSTRACT

The purpose of this study is to calculate diagnostic accuracy of chronic lateral ankle instability (CLAI) from a confusion matrix using deep learning (DL) on ultrasound images of anterior talofibular ligament (ATFL). The study included 30 ankles with no history of ankle sprains (control group), and 30 ankles diagnosed with CLAI (injury group). A total of 2000 images were prepared for each group by capturing ultrasound videos visualizing the fibers of ATFL under the anterior drawer stress. The images of 20 feet in each group were randomly selected and used for training data and the images of remaining 10 feet in each group were used as test data. Transfer learning was performed using 3 pretraining DL models, and the accuracy, precision, recall (sensitivity), specificity, F-measure, and the area under the receiver operating characteristic curve (AUC) were calculated based on the confusion matrix. The important features were visualized using occlusion sensitivity, a method for visualizing areas that are important for model prediction. DL was able to diagnose CLAI using ultrasound imaging with very high accuracy and AUC in three different learning models. In visualization of the region of interest, AI focused on the substance of the ATFL and its attachment on the fibula for the diagnosis of CLAI.

1. Introduction

Anterior talofibular ligament (ATFL) is the most commonly injured ligament in ankle sprains because of its anatomical position.[1] However, if not properly diagnosed and treated initially, ATFL injuries can become chronic and require surgical treatment as chronic lateral ankle instability (CLAI). CLAI may occur in about 10–20 % of patients after ankle sprains such as ATFL injury.[2,3] CLAI is a chronic condition that presents with symptoms such as pain, persistent swelling, feelings of ankle instability and giving-way, may cause an inability to participate in work and sports.[4,5] To correctly diagnose ankle instability, a combination of physical findings and imaging examinations are used after obtaining the patient's medical history. The traditional physical examination test for the evaluation of the ankle instability is the anterior drawer test (ADT), which evaluates anterior talus displacement against an anteriorly orientated force, and control of ankle plantarflexion to tense the lateral ligament. However, due to the poor reliability of the physical diagnosis of ankle instability, magnetic resonance imaging (MRI) and stress radiography are commonly performed in combination.[6,7] MRI has been shown to have high specificity and high sensitivity for ATFL tears, especially in the acute phase,[8] and has been used to evaluate soft tissue conditions such as ATFL tears or thickening in the diagnosis of CLAI, but is not optimal for assessing the ankle instability because it is a static examination.[9] Although stress radiography is a useful test to evaluate ankle instability, it is a complicated procedure, and results depend on the position of the patient's foot, the magnitude of the force applied to the foot, and the ability of the patient to withstand the force.[10]

Along with the recent development of ultrasound technology, ultrasound has become a very useful tool in the diagnosis of soft tissue injuries, especially in the ankle-foot region, and has even become the one of the gold standard examinations. When imaging the ankle, ultrasound is able to detect synovial lesions, ligamentous injury, and distinguish soft tissue from osseous impingement.[8] Furthermore, the dynamic assessment is another advantage of ultrasound, and many studies have

* Corresponding author. Department of Orthopaedic Surgery, Kobe University Graduate School of Medicine, 7-5-1 Kusunoki-cho, Chuo-ku, Kobe, 650-0017, Japan.
E-mail addresses: ocumctb13@gmail.com (M. Kamachi), koheikamada1202@gmail.com (K. Kamada), kanzaki@med.kobe-u.ac.jp (N. Kanzaki), ytetsu36@gmail.com (T. Yamamoto), you.1.hoshino@gmail.com (Y. Hoshino), ainui@med.kobeu.ac.jp (A. Inui), y.n.fuzuki18@gmail.com (Y. Nakanishi), k.nishida19830610@gmail.com (K. Nishida), kantona9@gmail.com (K. Nagai), matsushi@med.kobe-u.ac.jp (T. Matsushita), kurodar@med.kobe-u.ac.jp (R. Kuroda).

https://doi.org/10.1016/j.asmart.2025.01.001
Received 9 July 2024; Received in revised form 8 January 2025; Accepted 12 January 2025
Available online 22 January 2025

reported that ultrasound imaging and dynamic assessment of ATFL are useful in the diagnosis of CLAI.[6,10–15] Although the diagnostic parameters of ATFL for the diagnosis of CLAI have not yet been established, several studies demonstrated that the change in ATFL length of manual stress ultrasound could be useful for diagnosis of CLAI.[6,10,12] On the other hand, some studies have found it useful to assess the thickness of the ATFL,[13–15] there is no certain consensus on the ultrasound diagnosis of CLAI. Therefore, this study focuses on the application of deep learning (DL) technology to ultrasound images.

Recently, artificial intelligence (AI) has developed remarkably and has been rapidly applied in the medical research field. DL using convolutional neural networks (CNNs) which is an AI method has been adapted to clinical practice, particularly in the diagnostic imaging field, with even reaching superhuman performance at certain image interpretation tasks.[16] With the help of DL algorithms, such as artificial neural networks and CNNs, AI has been able to improve diagnostic accuracy and speed, reduce the amount of human error, reduce the strain on medical professionals, and improve care. Regarding research using DL in the field of orthopaedics, the accuracy of the AI to detect pathologies were reported as equivalent or even superior to humans in several imaging modalities, such as radiography, MRI and ultrasound.[17–22] Despite the increasing usefulness of ultrasound, as mentioned above, there has been no research on the use of DL for musculoskeletal ultrasound imaging in the field of ankle-foot. Therefore, the purpose of this study is to calculate diagnostic accuracy of CLAI from a confusion matrix using DL on ultrasound images of ATFL. The hypothesis of this study is that the application of DL to US images of ATFL will enable the diagnosis of CLAI more accurately and easily than conventional methods such as MRI. Furthermore, we investigated the possibility of obtaining useful information for the diagnosis of CLAI by visualizing areas that may be important.

2. Materials and methods

This study was approved by the appropriate review board (No. B210049), and informed consent was obtained from all patients involved. The study included 30 ankles consisting of the healthy volunteers and the patients (25 persons, 14 males and 11 females) with no history of ankle sprains (control group), and 30 ankles consisting of 26 patients (16 males and 10 females) who were diagnosed with CLAI and later underwent arthroscopic lateral ligament repair (injury group). Postoperative patients, patients with foot deformities and those with general laxity were excluded. The mean age of the control group was 34.8 ± 10.6 years old (range: 17–47 years old), and the mean age of the injury group was 31.9 ± 12.7 years old (range:13–59 years old). CLAI was comprehensively diagnosed by a certified ankle-foot surgeon based on patient's history, physical examination, stress radiographs, ultrasound images, and MRI. The sample size was determined by power analysis based on historical data using G*Power 3.1. There was a significant difference of 0.5 cm in length change of ATFL between healthy volunteers and patients with CLAI in the previous report.[10] A prior sample size calculation revealed that a difference of 0.5 cm in length change of ATFL would be detectable between two groups with a sample size of 25 in each group by using the *t*-test (effect size = 0.95, with an α of 0.05 and a power of 0.95). Therefore, the sample size for this study was set at 30 feet in each group.

2.1. Ultrasound examination

Ultrasound imaging was performed by an ankle-foot expert with 10 years of musculoskeletal ultrasound imaging experience. A long-axis image of the ATFL using an 18M linear probe (Canon APLIO300, TUS-A300, Canon Medical Systems, Tochigi, Japan) were obtained according to previous reports.[6,10,23] The ultrasound settings of gain, dynamic range, and frame rate were standardized for all measurements. Specifically, the gain was set to 80 dB, the dynamic range to 70 dB, and the frame rate to 60 fps. The transducer was placed over the ATFL according to the following steps; the proximal edge of the transducer was adjusted on the distal edge of the lateral malleolus of the ankle, and the distal end of the transducer was then turned carefully parallel to the sole of foot to visualize the fibers of ATFL clearly. Each patient was in a sitting position with one's heel hanging on the stool. To apply anterior stress to the ankle joint during ultrasound examination, the reverse anterior drawer test[24] was performed by pushing the lower leg in with one hand (Fig. 1).

2.2. Data preparation

Ultrasound movies applying anteriorly directed force to the ankle joint were captured with the transducer held on the ATFL. A total of 2000 images with maximum anterior stress were prepared for each group by capturing images from the movies. Dynamic ultrasound imaging of the ATFL was performed, capturing its progression from a relaxed state to maximum anterior drawer stress. From the recorded video, a still image (128 pixels × 128 pixels) representing the maximum stress condition was extracted. A 35 × 20 mm area, including the lateral malleolus, ATFL, and the talus, was cropped and then used for DL. DL was performed using the Deeplearning Toolbox of MATLAB (MathWorks, Natick, MA), and the images of 20 feet in each group were randomly selected and used for training data. The images of remaining 10 feet in each group were used as test data. As a preprocessing step, the ImageAugmentor tool in MATLAB was used to increase the variation in the original dataset by applying horizontal flipping, rotation (−10°–10°), scaling (× 0.8 to × 1.2), horizontal translation, vertical translation, and random sharing to train images and augmented the validation images.

2.3. Training and test process of deep learning

Training and test process of deep learning was performed in a method based on a previous report.[25] Flowchart of the deep leaning process was shown in Fig. 2. Transfer learning was performed using 3 pretraining DL models (Residual Net (ResNet)-50, MobileNet_v2, and EfficientNet) that are commonly used in medical imaging. ResNet-50: A 50-layer deep neural network leveraging residual connections, designed for high accuracy and robust performance on large-scale tasks, though it requires substantial computational resources. MobileNet_V2: A lightweight model tailored for mobile and edge devices, employing depthwise separable convolutions and inverted residual blocks to maximize efficiency, with a slight trade-off in accuracy. EfficientNet: A scalable model that optimizes accuracy and efficiency through compound scaling of depth, width, and resolution, making it versatile for both mobile and server-side applications. These models used different numbers of convolutional layers: 50 in ResNet-50, 53 in MobileNet_v2, and 82 in EfficientNet. The accuracy of each DL model was assessed using a confusion matrix, a table containing four combinations of predicted and actual values for the presence or absence of disease. The values in the matrix include true positives, false positives, true negatives, and false negatives (Fig. 3). For each learning model, the accuracy (percentage of correct answers for all data), precision (percentage of AI correctly judged CLAI group), recall (percentage of data correctly judged by AI as CLAI group, same as sensitivity), specificity (percentage of data correctly judged by AI as control group), and F-measure (the harmonic mean of the accuracy and recall), which are widely used in the field of machine learning, were calculated based on the confusion matrix.[25,26] The important features detected by the network were visualized using occlusion sensitivity, a method for visualizing areas that are important for model prediction. Occlusion sensitivity displays a heat map of regions that are important for the AI to judge control or CLAI on test data. Furthermore, the area under the receiver operating characteristic curve (AUC) was calculated by plotting the true-positive and false-positive rates on the coordinate axes. The 95 % confidence intervals (CIs) for accuracy, precision, recall (sensitivity), specificity, and AUC were calculated using the bootstrap

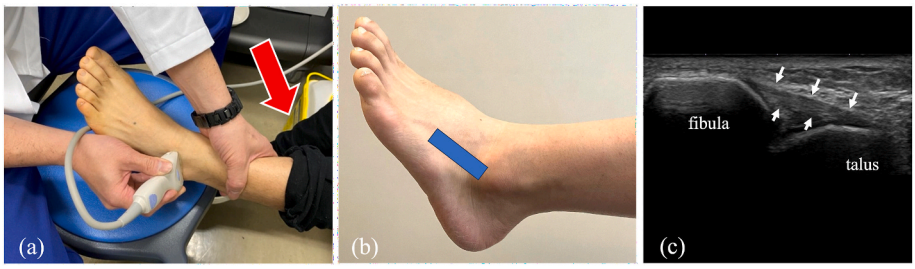

Fig. 1. (a) The transducer was placed sequentially over the ATFL under the condition of anterior drawer stress by reverse anterior drawer test. (Red arrows: direction of force) (b) The positioning of the transducer. (C)long-axis ultrasound image of the ATFL under the condition of anterior drawer stress. (White arrows: ATFL).

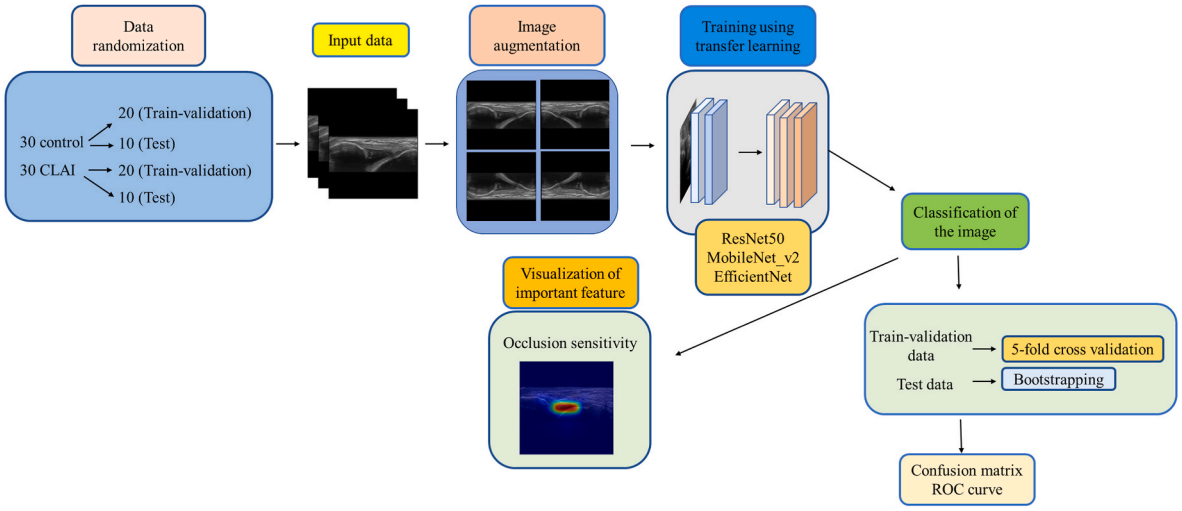

Fig. 2. Flowchart of the deep leaning process.

(a)

Predicted class	True class: CLAI	True class: control
CLAI	True Positive (TP)	False Positive (FP)
control	False Negative (FN)	True Negative (TN)

(b)

Accuracy= (TP+TN)/ (TP+FP+FN+TN)
Precision= TP/ (TP+FP)
Recall (sensitivity) = TP/ (TP+FN)
Specificity=TN/ FP+TN
F.Measure= 2* (Precision*Recall)/ (Precision + Recall)

Fig. 3. (a) A confusion matrix, a table containing four combinations of predicted and Actual values for the presence or absence of disease. (b) Diagnostic accuracy from the learning model is calculated from the confusion matrix.

method.[27]

3. Results

For each model, the diagnostic accuracy was evaluated based on the confusion matrix obtained from the test data (Table 1). From the confusion matrix, the diagnostic accuracy of ResNet-50 was 0.989 (95 % CI: 0.989–0.991), MobileNet_v2 was 0.972 (CI 0.971–0.973), and EfficientNet was 0.980 (CI 0.979–0.981), all networks showed very high accuracy. The AUC, which is a plot of the true positive rate and false positive rate on the coordinate axis, was 0.998 for ResNet, 0.995 for MobileNet_v2, and 0.999 for EfficientNet (Fig. 4). DL was able to diagnose CLAI using ultrasound imaging with very high accuracy and AUC in three different learning models.

According to occlusion sensitivity, the important feature that the AI had detected was visualized using an overlaid heatmap. As a result of this study, it was found that AI focused on the substance of the ATFL and its attachment on the fibula for the diagnosis of CLAI (Fig. 5).

4. Discussion

The most important finding of this study is that DL was able to diagnose CLAI using ultrasound imaging with very high accuracy and AUC in three different learning models. Furthermore, in visualization of the

Table 1
Diagnostic accuracy from the learning model was calculated from the confusion matrix created from testing data. (95 % confidence interval.)

Network	Accuracy	Precision	Recall (Sensitivity)	Specificity	F-Measure
ResNet-50	0.989 (0.989–0.991)	1.00	0.980 (0.979–0.981)	0.981 (0.980–0.982)	0.990 (0.989–0.991)
MobileNet_v2	0.972 (0.971–0.973)	0.968 (0.967–0.971)	0.975 (0.973–0.977)	0.974 (0.973–0.975)	0.972 (0.971–0.973)

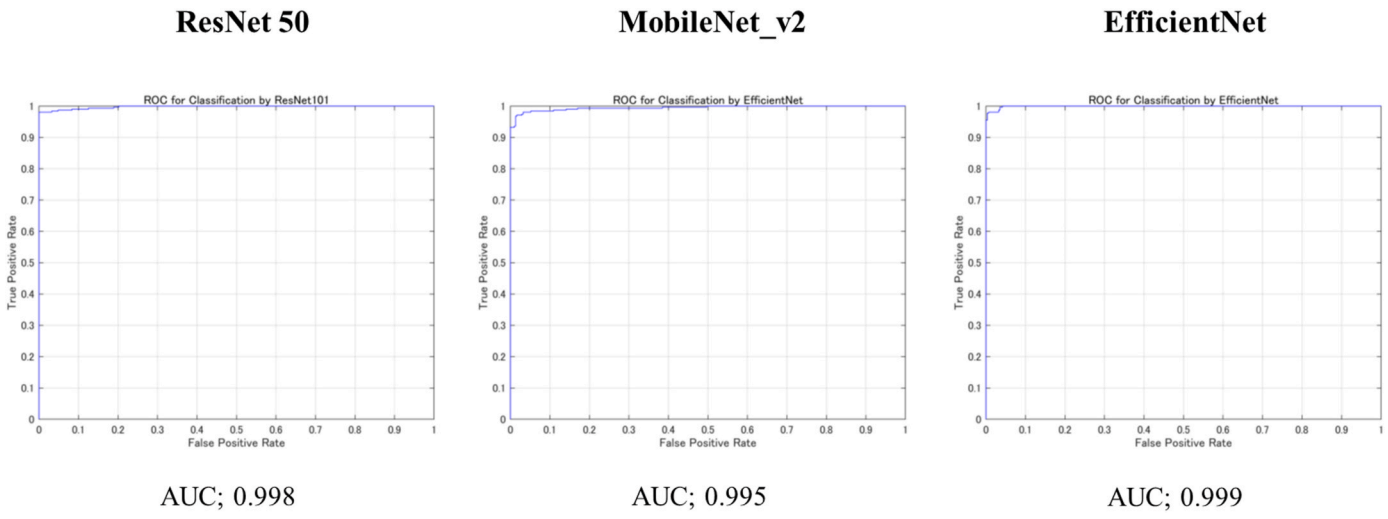

Fig. 4. Area under the curves (AUC) of each learning models based on the receiver operating characteristic (ROC) curve.

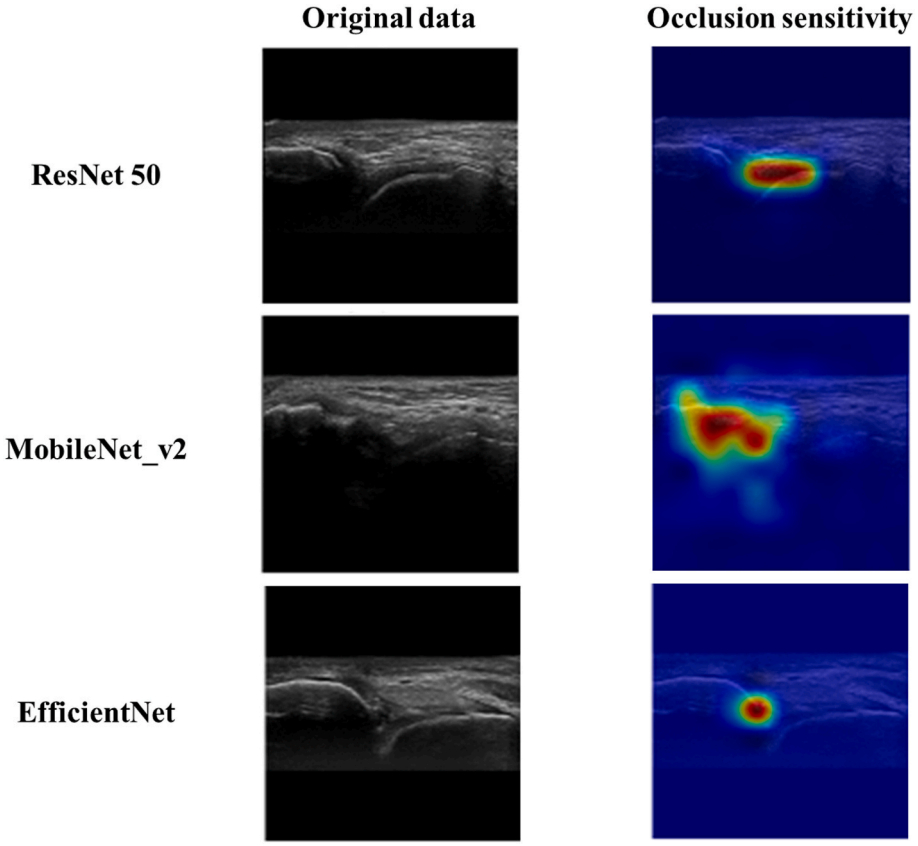

Fig. 5. Visualization of the region of interest using occlusion sensitivity. The heatmap shows the areas that are important for the AI to judge control or CLAI on the test data.

region of interest, AI focused on the substance of the ATFL and its attachment on the fibula for the diagnosis of CLAI.

In recent years, ultrasound imaging has become increasingly important in the evaluation of soft tissue injuries because of its dynamic diagnostic capability. Ultrasound has been considered particularly useful in the field of ankle and foot, and there have been many studies on ultrasound diagnosis of CLAI.[6,7,10–15,28,29] In 2016, Radwan et al. reported an accuracy of 87~90.9 %, sensitivity of 84.6–100 %, and specificity of 90.9–100 % for ultrasound diagnosis of CLAI in a Systematic review including six high-quality studies.[30] Furthermore, in 2020, Lee et al. reported an accuracy of 0.96 for CLAI ultrasound in a Systematic review including 10 studies with a reference standard of operative finding.[31] Regarding previous reports which investigated individual parameters of ultrasound imaging of CLAI, several studies have focused on changes in ATFL length with and without stress.[6,10,12] Using ultrasound images of the ATFL taken at rest and in the maximal anterior drawer position, Lee et al. reported that the ratio of ATFL length with and without stress (ATFL ratio) is useful for the diagnosis of CLAI.[6] Cho et al. similarly demonstrated that the change in ATFL length of manual stress ultrasound could be used for diagnosis of chronic ankle instability.

On the other hand, Liu compared the healthy and unstable ankle joints by ultrasound imaging and found that the anterior talofibular ligament of the previously sprained ankle was thicker than those of the uninjured ankle,[13] and Abdeen et al. also reported the length and the thickness of the ATFL were longer and thicker in injured groups compared to healthy.[15] However, measuring length and thickness of ATFL by ultrasound is cumbersome and time consuming, and there is still no consistent consensus on those parameters in the diagnosis of CLAI. As it is reported that the reliability of the ATFL delineation and length measurement seems to be highly dependent on the experience and skill of the examiner in ultrasound diagnosis,[32] it is not easy to perform an anterior drawer test while accurately delineating the ATFL with ultrasound. In this study, the reverse anterior drawer test[24] was used, in which the patient's heel is placed on a stool and the lower leg is pushed in to apply an anterior drawer stress. Since this method can apply anterior drawer stress relatively easily with one hand, it is suitable with ultrasonography, which requires holding the transducer with the other hand, and allows even inexperienced examiners to perform the test accurately and easily. It is important to accurately delineate the ATFL and reproducibly apply adequate anterior drawer stress for the accurate diagnosis of CLAI, and these ingenuities of the examination may have contributed to the very high diagnostic accuracy in this study.

In order to eliminate the uncertainty factors caused by the ultrasound examination, this study attempted to apply DL technology, which automatically learns image features.[33] With the rapid development of AI technology in recent years, DL has been widely applied in medicine, especially in the field of diagnostic imaging. Ultrasound has advantages such as non-ionizing, low-cost, portable, point-of-care, and real-time imaging, and the growing need for efficient and objective acquisition and evaluation of ultrasound images has led to a recent trend toward the maturation of AI enabled ultrasound diagnostics, which is approaching routine clinical applications.[34] Research on DL for ultrasound images is ongoing in the field of breast surgery.[22,35] Han et al. exploited the deep learning framework to differentiate the distinctive types of lesions and nodules in breast acquired with ultrasound imaging. GoogLeNet convolutional neural network was trained to distinguish between benign and malignant tumors, showing an area under the curve of over 0.9, an accuracy of about 0.9 (90 %), a sensitivity of 0.86, and a specificity of 0.96.[35] In a similar DL study using ultrasound images for the diagnosis of malignant breast cancer, the AUC (0.913) was reported to be higher than the AUC obtained by sonographers (0.846) in the best learning model.[22] Shinohara et al. found in a recent study that ultrasound images using the DL model predicted triangular fibrocartilage complex injury with high accuracy, with the best scores of 0.85 for accuracy on GoogLeNet, 1.00 for sensitivity on ResNet50 and ResNet101, and 0.78 for specificity on GoogLeNet.[26] Shinohara et al. also reported high diagnostic accuracy using a similar technique of DL in ultrasound imaging of cubital tunnel syndrome.[25] These reports are an attempt to utilize AI technology to improve diagnostic accuracy for diseases for which ultrasound has been used as an assistive diagnostic modality, without involving patient invasion. In the present study, very high accuracy and AUC results were obtained by using DL for ultrasound images in CLAI, which ultrasound is used as an adjunct diagnosis. The combination of ultrasound and AI, which enables non-invasive, low-cost, point-of-care for patients, has room for further development and may play an important role in the future of diagnostic imaging.

Although accuracy is essential in AI-based diagnostic imaging technology, the basis for model decision making must be understandable to humans. In this regard, occlusion sensitivity is a very interesting technology that can effectively visualize multifocal glass opacities and consolidations and visualize important image features in detail.[36] This visualization tool may provide the necessary information for diagnosis by highlighting the basis for predictions made by the DL model. The results of this study indicate that AIs focus on the substance of the ATFL and its attachment to the fibula in the diagnosis of CLAI. The results are very interesting and suggest that AI has the potential to assess the subtle post-injury changes at the fibular attachment site and the quality of the substance of the ATFL, although we often assess relative talar mobility with the anterior drawer test in routine practice of CLAI diagnosis.

In the future, if ATFL ultrasound imaging techniques and settings can be standardized, it could enable effective diagnosis of CLAI across various patient groups and other facilities. Consistent imaging protocols would help ensure that the diagnostic process is applicable and reliable in a wider range of clinical environments.

AI-based deep learning offers the ability to recognize image features from angles that may not be immediately visible to human clinicians. Unlike traditional diagnostic methods that depend on expert analysis, deep learning can identify intricate patterns within the data, revealing subtle elements that might not be easily quantified. This unique ability allows for a deeper understanding of ultrasound images, potentially leading to more precise and consistent diagnoses of CLAI. Additionally, deep learning models, trained on large and varied datasets, could enhance their adaptability to different clinical settings and patient populations. Using AI in this manner not only promises to improve diagnostic precision but could also highlight previously unrecognized aspects of the condition, ultimately advancing patient care.

This study has the following limitations. First, the results were obtained on ultrasound images; generalization of the model's performance to images from other diagnostic instruments was not investigated. Second, no comparison of accuracy with other diagnostic devices was performed. Third, although many images were examined, the number of cases studied was not large. Fourth, this study was conducted with static images under the anterior drawer stress, and originally stressed examinations should be examined with video images. We are in the process of developing a study applying AI to video. Video has the advantage of capturing dynamic information, easily tracking the movement of ligaments, and providing a large amount of data. However, it also has the disadvantage of requiring more time for analysis due to the large data volume and the noise caused by movement, which can affect the accuracy of the analysis. On the other hand, images offer the advantage of efficient processing, the ability to select noise-free frames, and easier image manipulation. However, they lack the ability to provide dynamic information. Fifth, the studies all used the same ultrasound equipment and all images were obtained by a single examiner. To improve generalizability, it is necessary to validate the accuracy of the measurements by adding data obtained from different examiners on different equipment.

5. Conclusions

DL was able to diagnose CLAI using ultrasound imaging with very high accuracy and AUC in three different learning models. Furthermore, in visualization of the region of interest, AI focused on the substance of the ATFL and its attachment on the fibula for the diagnosis of CLAI. Concerning clinical relevance, this method utilizing DL can be improved in the future to provide a more convenient and accurate diagnosis of CLAI using ultrasound imaging, which is minimally invasive and low cost.

Informed consent

Informed consent was obtained from all the participants.

Funding

This research received no external funding.

Conflict of interest

The authors declared that there is no conflict of interest.

Acknowledgments

This study has no acknowledgement.

References

1. Salat P, Le V, Veljkovic A, Cresswell ME. Imaging in foot and ankle instability. *Foot Ankle Clin*. 2018;23(4). https://doi.org/10.1016/j.fcl.2018.07.011.
2. Chandnani VP, Harper MT, Ficke JR, et al. Chronic ankle instability: evaluation with MR arthrography, MR imaging, and stress radiography. *Radiology*. 1994;192(1). https://doi.org/10.1148/radiology.192.1.8208935.
3. Konradsen L, Bech L, Ehrenbjerg M, Nickelsen T. Seven years follow-up after ankle inversion trauma. *Scand J Med Sci Sports*. 2002;12(3). https://doi.org/10.1034/j.1600-0838.2002.02104.x.
4. Gribble PA, Bleakley CM, Caulfield BM, et al. Evidence review for the 2016 International Ankle Consortium consensus statement on the prevalence, impact and long-term consequences of lateral ankle sprains. *Br J Sports Med*. 2016;50(24). https://doi.org/10.1136/bjsports-2016-096189.
5. Vuurberg G, Hoorntje A, Wink LM, et al. Diagnosis, treatment and prevention of ankle sprains: update of an evidence-based clinical guideline. *Br J Sports Med*. 2018;52(15). https://doi.org/10.1136/bjsports-2017-098106.
6. Lee KT, Park YU, Jegal H, Park JW, Choi JP, Kim JS. New method of diagnosis for chronic ankle instability: comparison of manual anterior drawer test, stress radiography and stress ultrasound. *Knee Surg Sports Traumatol Arthrosc*. 2014;22(7). https://doi.org/10.1007/s00167-013-2690-x.
7. Oae K, Takao M, Uchio Y, Ochi M. Evaluation of anterior talofibular ligament injury with stress radiography, ultrasonography and MR imaging. *Skeletal Radiol*. 2010;39(1). https://doi.org/10.1007/s00256-009-0767-x.
8. S. J, U. A, S. C, B. S, K. H. Accuracy of MRI scan in the diagnosis of ligamentous and chondral pathology in the ankle. *Foot Ankle Surg*. 2010;16(2).
9. Hua J, Xu JR, Gu HY, et al. Comparative study of the anatomy, CT and MR images of the lateral collateral ligaments of the ankle joint. *Surg Radiol Anat*. 2008;30(4). https://doi.org/10.1007/s00276-008-0328-3.
10. Cho JH, Lee DH, Song HK, Bang JY, Lee KT, Park YU. Value of stress ultrasound for the diagnosis of chronic ankle instability compared to manual anterior drawer test, stress radiography, magnetic resonance imaging, and arthroscopy. *Knee Surg Sports Traumatol Arthrosc*. 2016;24(4). https://doi.org/10.1007/s00167-015-3828-9.
11. Hua Y, Yang Y, Chen S, Cai Y. Ultrasound examination for the diagnosis of chronic anterior talofibular ligament injury. *Acta Radiol*. 2012;53(10). https://doi.org/10.1258/ar.2012.120171.
12. Mizrahi DJ, Nazarian LN, Parker L. Evaluation of the anterior talofibular ligament via stress sonography in asymptomatic and symptomatic populations. *J Ultrasound Med*. 2018;37(8). https://doi.org/10.1002/jum.14542.
13. Liu K, Gustavsen G, Royer T, Wikstrom EA, Glutting J, Kaminski TW. Increased ligament thickness in previously sprained ankles as measured by musculoskeletal ultrasound. *J Athl Train*. 2015;50(2). https://doi.org/10.4085/1062-6050-49.3.77.
14. Yildizgoren MT, Velioglu O, Demetgul O, Turhanoglu AD. Assessment of the anterior talofibular ligament thickness in patients with chronic stroke: an ultrasonographic study. *J Med Ultrasound*. 2017;25(3). https://doi.org/10.1016/j.jmu.2017.03.001.
15. Abdeen R, Comfort P, Starbuck C, Nester C. Ultrasound characteristics of foot and ankle structures in healthy, coper, and chronically unstable ankles. *J Ultrasound Med*. 2019;38(4). https://doi.org/10.1002/jum.14770.
16. Shin HC, Roth HR, Gao M, et al. Deep convolutional neural networks for computer-aided detection: CNN architectures, dataset characteristics and transfer learning. *IEEE Trans Med Imag*. 2016;35(5). https://doi.org/10.1109/TMI.2016.2528162.
17. Olczak J, Fahlberg N, Maki A, et al. Artificial intelligence for analyzing orthopedic trauma radiographs: deep learning algorithms—are they on par with humans for diagnosing fractures? *Acta Orthop*. 2017;88(6). https://doi.org/10.1080/17453674.2017.1344459.
18. Chung SW, Han SS, Lee JW, et al. Automated detection and classification of the proximal humerus fracture by using deep learning algorithm. *Acta Orthop*. 2018;89(4):468–473. https://doi.org/10.1080/17453674.2018.1453714.
19. Kunze KN, Rossi DM, White GM, et al. Diagnostic performance of artificial intelligence for detection of anterior cruciate ligament and meniscus tears: a systematic review. *Arthrosc J Arthrosc Relat Surg*. 2021;37(2). https://doi.org/10.1016/j.arthro.2020.09.012.
20. Ma J, Wu F, Zhu J, Xu D, Kong D. A pre-trained convolutional neural network based method for thyroid nodule diagnosis. *Ultrasonics*. 2017;73. https://doi.org/10.1016/j.ultras.2016.09.011.
21. Xue Y, Zhang R, Deng Y, Chen K, Jiang T. A preliminary examination of the diagnostic value of deep learning in hip osteoarthritis. *PLoS One*. 2017;12(6). https://doi.org/10.1371/journal.pone.0178992.
22. Zhang H, Han L, Chen K, Peng Y, Lin J. Diagnostic efficiency of the breast ultrasound computer-aided prediction model based on convolutional neural network in breast cancer. *J Digit Imag*. 2020;33(5). https://doi.org/10.1007/s10278-020-00357-7.
23. Kemmochi M, Sasaki S, Fujisaki K, Oguri Y, Kotani A, Ichimura S. A new classification of anterior talofibular ligament injuries based on ultrasonography findings. *J Orthop Sci*. 2016;21(6). https://doi.org/10.1016/j.jos.2016.06.011.
24. Li Q, Tu Y, Chen J, et al. Reverse anterolateral drawer test is more sensitive and accurate for diagnosing chronic anterior talofibular ligament injury. *Knee Surg Sports Traumatol Arthrosc*. 2020;28(1). https://doi.org/10.1007/s00167-019-05705-x.
25. Shinohara I, Inui A, Mifune Y, et al. Diagnosis of cubital tunnel syndrome using deep learning on ultrasonographic images. *Diagnostics*. 2022;12(3). https://doi.org/10.3390/diagnostics12030632.
26. Shinohara I, Inui A, Mifune Y, et al. Ultrasound with artificial intelligence models predicted palmer 1B triangular fibrocartilage complex injuries. *Arthrosc J Arthrosc Relat Surg*. 2022;38(8). https://doi.org/10.1016/j.arthro.2022.03.037.
27. Matsuo H, Nishio M, Kanda T, et al. Diagnostic accuracy of deep-learning with anomaly detection for a small amount of imbalanced data: discriminating malignant parotid tumors in MRI. *Sci Rep*. 2020;10(1). https://doi.org/10.1038/s41598-020-76389-4.
28. Lee SH, Yun SJ. The feasibility of point-of-care ankle ultrasound examination in patients with recurrent ankle sprain and chronic ankle instability: comparison with magnetic resonance imaging. *Injury*. 2017;48(10). https://doi.org/10.1016/j.injury.2017.07.015.
29. Lee SH, Yun SJ. The feasibility of point-of-care ankle ultrasound examination in patients with recurrent ankle sprain and chronic ankle instability: comparison with magnetic resonance imaging. *Injury*. 2017;48(10). https://doi.org/10.1016/j.injury.2017.07.015.
30. Radwan A, Bakowski J, Dew S, Greenwald B, Hyde E, Webber N. Effectiveness of ultrasonography in diagnosing chronic lateral ankle instability:a systematic review. *Int J Sports Phys Therapy*. 2016;11(2).
31. Lee SH, Yun SJ. Ankle ultrasound for detecting anterior talofibular ligament tear using operative finding as reference standard: a systematic review and meta-analysis. *Eur J Trauma Emerg Surg*. 2020;46(1). https://doi.org/10.1007/s00068-019-01169-3.
32. Kristen KH, Seilern und Aspang J, Wiedemann J, Hartenbach F, Platzgummer H. Reliability of ultrasonography measurement of the anterior talofibular ligament (ATFL) length in healthy subjects (in vivo), based on examiner experience and patient positioning. *J Experimen Orthopaedics*. 2019;6(1). https://doi.org/10.1186/s40634-019-0199-z.
33. Apostolopoulos ID, Mpesiana TA. Covid-19: automatic detection from X-ray images utilizing transfer learning with convolutional neural networks. *Phy Eng Sci Med*. 2020;43(2). https://doi.org/10.1007/s13246-020-00865-4.
34. Akkus Z, Cai J, Boonrod A, et al. A survey of deep-learning applications in ultrasound: artificial intelligence–powered ultrasound for improving clinical workflow. *J Am Coll Radiol*. 2019;16(9). https://doi.org/10.1016/j.jacr.2019.06.004.
35. Han S, Kang HK, Jeong JY, et al. A deep learning framework for supporting the classification of breast lesions in ultrasound images. *Phys Med Biol*. 2017;62(19). https://doi.org/10.1088/1361-6560/aa82ec.
36. Prakash NB, Murugappan M, Hemalakshmi GR, Jayalakshmi M, Mahmud M. Deep transfer learning for COVID-19 detection and infection localization with superpixel based segmentation. *Sustain Cities Soc*. 2021;75. https://doi.org/10.1016/j.scs.2021.103252.